

RESEARCH ARTICLE

SHP-1 suppresses the antiviral innate immune response by targeting TRAF3

Doudou Hao¹ | Yu Wang^{2,3} | Liuyan Li¹ | Gui Qian¹ | Jing Liu¹ | Manman Li¹ | Yihua Zhang¹ | Ruixue Zhou¹ | Dapeng Yan¹

¹Department of Immunology, School of Basic Medical Sciences and Shanghai Public Health Clinical Center, Fudan University, Shanghai, China

²National Engineering Research Centre of Immunological Products, Department of Microbiology and Biochemical Pharmacy, College of Pharmacy, Army Medical University, Chongqing, China

³Department of Basic Courses, NCO School, Army Medical University, Shijiazhuang, China

Correspondence

Dapeng Yan, Department of Immunology, School of Basic Medical Sciences and Shanghai Public Health Clinical Center, Fudan University, Dong'an Road 130, Xuhui District, Shanghai 200032, China. Email: dapengyan@fudan.edu.cn

Funding information

National Natural Science Foundation of China (NSFC), Grant/Award Number: 31972900, 31670901 and 81871249; Shanghai Institutions of Higher Learning, Grant/Award Number: TP2016007; Outstanding Youth Training Program of Shanghai Municipal Commission of Health and Family Planning, Grant/Award Number: 2017YQ012; National Key Research and Development Program of China, Grant/Award Number: 2016YFC1305103 and 2018YFC1705505; National Megaproject on Key Infectious Diseases, Grant/Award Number: 2017ZX10202102

Abstract

Type I interferons play a pivotal role in innate immune response to virus infection. The protein tyrosine phosphatase SHP-1 was reported to function as a negative regulator of inflammatory cytokine production by inhibiting activation of NF- κ B and MAPKs during bacterial infection, however, the role of SHP-1 in regulating type I interferons remains unknown. Here, we demonstrated that knockout or knockdown of SHP-1 in macrophages promoted both HSV-1- and VSV-induced antiviral immune response. Conversely, overexpression of SHP-1 in L929 cells suppressed the HSV-1- and VSV-induced immune response; suppression was directly dependent on phosphatase activity. We identified a direct interaction between SHP-1 and TRAF3; the association between these two proteins resulted in diminished recruitment of CK1 ϵ to TRAF3 and inhibited its K63-linked ubiquitination; SHP-1 inhibited K63-linked ubiquitination of TRAF3 by promoting dephosphorylation at Tyr116 and Tyr446. Taken together, our results identify SHP-1 as a negative regulator of antiviral immunity and suggest that SHP-1 may be a target for intervention in acute virus infection.

KEYWORDS

immune signaling transduction, immunoregulation, protein-protein interaction, type I interferon, virus infection

Abbreviations: DAPI, 4',6-diamidino-2-phenylindole; HSV-1, herpes simplex virus 1; IFN, interferon; IRF3, interferon regulatory factor 3; MAVS, mitochondrial antiviral-signaling protein; Med, medium; MOI, multiplicity of infection; PAMPs, pathogen-associated molecular patterns; PRRs, pattern recognition receptors; qRT-PCR, quantitative real-time PCR; RIG-I, retinoic acid inducible gene-I; siRNA, small interfering RNA; STING, stimulator of interferon genes protein; TBK1, tank-binding kinase 1; TLRs, toll like receptors; TRAF3, tumor necrosis factor receptor associated factor; VSV, vesicular stomatitis virus.

Doudou Hao and Yu Wang contributed equally to this work.

1 | INTRODUCTION

Viruses, including human immunodeficiency virus (HIV)-1, Zika virus, Ebola virus, and influenza virus, are worldwide problems that threaten human health and result in enormous economic losses and social problems.¹⁻⁴ Emergence of the novel coronavirus, SARS-CoV-2, has resulted in an extraordinary public health crisis in China that is having an impact worldwide.⁵⁻⁷ At present, there is no effective means for prevention or specific treatment for this pathogen.⁸ As host innate immune response provides critical control of virus infection, an improved understanding of the molecular mechanisms that promote antiviral innate immunity will permit intervention at the earliest stages of infection.

As the first line of defense against invading viruses, host immune cells synthesize and secrete type I interferons (IFNs) including IFN- α and IFN- β ; these factors promote antiviral, anti-proliferative, and immunomodulatory functions. Type I IFNs are critical components of the innate defense against viral infections. Virus infection can activate antiviral signaling pathways including TBK1-IRF3 as well as NF- κ B and MAPK pathway.^{9,10} Viruses and their components induce type I IFN responses via the activation of pattern recognition receptors (PRRs),¹¹ notably the toll-like receptors (TLRs) which are detected both intracellularly and on the cell surface. TLRs 3, 7, 8, and 9 recognize virus-derived nucleic acids and activate signaling cascades that lead to translocation of the transcription factors NF- κ B, IRF3, and IRF7 into the nucleus; these signaling events result in the induction of type I IFNs.^{12,13} The retinoic acid inducible gene-1 (RIG-I) and melanoma differentiation-associated gene-5 (MDA5) recognize virus replication intermediates such as intracellular dsRNA and likewise activate NF- κ B and IRFs through the adaptor mitochondrial antiviral signaling (MAVS) to induce type I IFNs.¹⁴⁻¹⁶ Moreover, cyclic GMP-AMP synthase (cGAS) specifically recognizes cytosolic DNA and responds by producing cyclic GMP-AMP (cGAMP); cGAMP binds to and activates the stimulator of interferon genes (STING), which serves to recruit and activate (TANK)-binding kinase 1 (TBK1), resulting in phosphorylation, dimerization, and translocation of IRF3 and production of type I IFNs.¹⁷⁻²⁰

Tumor necrosis factor (TNF) receptor-associated factor 3 (TRAF3) is a member of the extensive TNF receptor-associated factor family and includes N-terminal RING finger, zinc finger, and C-terminal meprin and TRAF homology (MATH) domains.²¹ TRAF3 also participates in the antiviral innate immune response and promotes Myd88 and TRIF-dependent activation of NF- κ B, AP-1, IRF3, and IRF7 via interactions with TLRs.²² Furthermore, in RIG-I-like receptor signaling pathways, MAVS recruits and induces K63-linked polyubiquitination of TRAF3, leading to the activation of TBK1 and

IRF3.²³⁻²⁵ Likewise, in the cGAS-STING signaling pathway, TRAF3 binds to STING and TBK1, which induces phosphorylation and dimerization of IRF3; this leads to translocation of IRF3 from the cytoplasm to the nucleus and ultimately results in induction of type I IFNs and proinflammatory cytokines.²⁶ These cytokines subsequently induce transcription of numerous antiviral genes that mediate innate antiviral immune response.

The cytoplasmic protein tyrosine phosphatase (PTP), Src homology 2 domain-containing PTP (SHP)-1, encoded by *Ptpn6*, is mainly expressed in myeloid cells including neutrophils, dendritic cells (DCs), monocytes, macrophages, mast cells, and eosinophils. SHP-1 is involved in numerous cell functions including proliferation, survival, adhesion, chemotaxis, phagocytosis, and degranulation.²⁷ SHP-1 contains two Src homology (SH)2 domains and a PTP domain and binds to immunoreceptor tyrosine-based inhibition motif-containing proteins, including FcRIIb, carcinoembryonic antigen cell adhesion molecule-1 (CD66a), and platelet and endothelial cell adhesion molecule-1 (CD31) to serve as negative regulator in multiple immune signaling pathways.²⁸ SHP-1 deficient mice (*Ptpn6*^{me-v/me-v}) display spontaneous and severe inflammatory and autoimmune diseases, indicating that SHP-1 is a key regulator of immune cell function. Our previous results showed that SHP-1 suppresses NF- κ B and MAPK signaling transduction in response to infection with enterohemorrhagic *Escherichia coli* by inhibiting K63-linked polyubiquitination of transforming growth factor beta-activated kinase 1.^{29,30} It is not yet clear whether SHP-1 participates in virus infection and can promote antiviral immune responses.

In this study, we examined the role of SHP-1 in the innate immune response to DNA or RNA virus and found that SHP-1 functioned as a negative regulator of antiviral signal transduction and thereby inhibited the synthesis of type I IFNs and proinflammatory cytokines promoted by virus infection. Mechanistically, our findings revealed a direct interaction between SHP-1 and TRAF3 that suppressed K63-linked ubiquitination of TRAF3 by dephosphorylating TRAF3 at Tyr116 and Tyr446. These findings reveal a previously unknown mechanism by which SHP-1 negatively regulates the posttranslational modifications of TRAF3 and suggests a molecular target for developing new therapeutics to limit the impact of acute virus infection.

2 | MATERIALS AND METHODS

2.1 | Cell culture

Primary mouse PMs as well as cells from the mouse macrophage line (RAW264.7; American Type Culture Collection (ATCC) TIB-71), cells from the mouse fibroblast line (L929, ATCC CCL-1), African green monkey kidney cells

(Vero, ATCC CCL-81) and cells from the human embryonic kidney (HEK293T, ATCC CRL-1573) were maintained in Dulbecco's modified Eagle's medium (DMEM; Hyclone) supplemented with 10% (v/v) of heat-inactivated FBS (Gibco) and 100 U/mL of penicillin and streptomycin (Hyclone). Cells from the human cervical cancer line (HeLa, ATCC CCL-2) were cultured in Roswell Park Memorial Institute 1640 medium (Hyclone) supplemented with 10% (v/v) of heat-inactivated FBS (Gibco) and 100 U/mL of penicillin and streptomycin (Hyclone). All the cells were incubated at 37°C with 5% of CO₂.

2.2 | Mouse strains

Mice heterozygous for SHP-1 deficiency ('motheaten' C57BL/6J *Ptpn6*^{me-v/+}/J mice; 000811; Jackson Laboratories) were bred in specific pathogen-free conditions at the Shanghai Research Center for Biomodel Organisms. Three-week-old homozygous *Ptpn6*^{me-v/me-v} mice and their WT littermates (control mice) were used in the experiments. All animal studies were approved by the Institutional Animal Care and Use Committee of the Fudan University.

2.3 | Isolation of mouse PMs

Three-week-old homozygous *Ptpn6*^{me-v/me-v} mice and their WT littermates were injected intraperitoneally (ip) with 1 mL of Brucella Broth (3%). Three days later, peritoneal lavage fluid was collected from the mice. Cells from the lavage fluid were collected by centrifugation and were washed three times in phosphate-buffered saline (PBS). PMs were cultured in DMEM supplemented with 10% of FBS and 100 U/mL of penicillin and streptomycin for 4 hours. Supernatants were removed, and PMs were cultured in DMEM without serum overnight prior to virus infection.

2.4 | Virus, virus infection, and titration

HSV-1 and VSV were collected from supernatants of infected Vero cells at the appearance of cytopathic effect. Virus titers in the supernatants were determined by standard plaque assay, and stocks were stored at -80°C. PMs, L929 cells, and HEK293T cells were incubated for 12 hours without serum, and then, infected with HSV-1 (multiplicity of infection (MOI) = 5) or VSV (MOI = 1) for the periods of time indicated.

2.5 | Reagents and antibodies

Primary antibodies included anti-phospho-TBK1 (CST, 3504), anti-phospho-IRF3 (CST, 29047), anti-phospho-STAT1

(CST, 9167), anti-phospho-p65 (CST, 3033), anti-phospho-p38 (CST, 9215), anti-phospho-Erk1/2 (CST, 9101), anti-SHP-1 (Abcam, 55356), anti-GAPDH (Sigma, SAB2108266), anti-HA (Sigma, H6908), anti-Flag (Sigma, F7425), anti-GST (CWBIO, CW0085M), and anti-His (CWBIO, CW0083M). Secondary antibodies included Alexa Fluor^R594 goat anti-rabbit IgG (Invitrogen, SA11012s) and Alexa Fluor^R488 goat anti-mouse IgG (Invitrogen, SA11001s). Some experiments included monoclonal mouse anti-Flag M2 Affinity Gel (Sigma, A2220) and protein A/G PLUS-Agarose (Santa Cruz, SC-2003).

2.6 | Plasmids and transfection

Plasmids encoding HA-ubiquitin, HA-CK1 ϵ , Flag-TRAF3, Flag-RIG-I, Flag-N-RIG-I, Flag-TBK1, and Flag-IRF3 were obtained from Dr B. Ge (Tongji University, Shanghai, China). HA-SHP-1^{C453S}, Flag-TRAF3 with mutations in Tyr residues, and individual domains of Flag-TRAF3 and Flag-SHP-1 were generated using KOD plus Mutagenesis Kit (SMK101, TOYOBO) according to the manufacturer's instructions. Plasmids encoding SHP-1 and MAVS were constructed into by PCR amplification and subcloning into pcDNA3.1. The genes encoding TRAF3 and SHP-1 were amplified by PCR and subcloned into pGEX-4T1 (Amersham) and pET28a (Novogen) vectors, respectively. HEK293T cells were transiently transfected using polyethylenimine (PEI; 23966-2; Polysciences) according to the manufacturer's instructions. L929 and HeLa cells were transiently transfected with Lipofectamine 2000 (11668; Invitrogen) according to the manufacturer's instructions.

2.7 | Immunoprecipitation and western blot

Forty-eight hours after transfection, HEK293T cells were washed three times with ice-cold PBS and lysed with lysis buffer (Beyotime) supplemented with 1% of protease inhibitor cocktail (B14002; Selleck), 1 mM of phenylmethylsulfonyl fluoride, 1 mM of NaF, and 1 mM of Na₃VO₄ on ice for 30 minutes. Cell lysates were centrifuged at 13,200 rpm for 15 minutes at 4°C. The supernatants were incubated with anti-Flag M2 Affinity Gel or anti-HA Affinity Gel at 4°C overnight. The samples equilibrated with affinity gels were centrifuged at 1000 rpm for 5 minutes at 4°C and washed three times with ice-cold PBST buffer (1% of Triton X-100 in PBS). The precipitates and lysates were boiled in 1 × sodium dodecyl sulfate (SDS) loading buffer for 10 minutes at 100°C. Proteins were separated by SDS-polyacrylamide gel electrophoresis and transferred onto polyvinylidene fluoride membranes soaked in methanol before, followed by blocking in Tris-buffered saline with 1% of Triton X-100 (TBST) with 5% of skim milk. After

washing three times, each for 5 minutes with TBST, the membranes were incubated with primary antibodies at 4°C overnight. Then, the membranes were incubated with HRP-linked secondary antibody for 2 hours after and washed as above. Proteins were visualized by enhanced chemiluminescence according to the manufacturer's instructions.

2.8 | Glutathione-S-transferase pull-down

The GST-TRAF3 and GST-control plasmids were transformed into BL-21 (DE3) (Tiangen Biotech) bacteria and induced to express GST fusion proteins at 30°C by isopropyl β-D-1-thiogalactopyranoside. GST fusion proteins were equilibrated with glutathione beads for 4 hours at 4°C and incubated with purified His-SHP-1 through Ni-column from BL-21 strain or lysates from mouse PMs. The beads were centrifuged at 1000 rpm for 5 minutes at 4°C and washed for three times, followed by boiling in 1 × SDS loading buffer for 10 minutes at 100°C and analyzed by immunoblot.

2.9 | Dual-luciferase reporter assay

HEK293T cells were seeded in 12-well plate and transiently transfected with IFN-β-Luc or ISRE-Luc, TK, and indicated plasmids for 24 hours. Luciferase activity was detected using the dual-luciferase reporter assay system (RG028; Beyotime) according to the manufacturer's instructions.

2.10 | Cell staining and confocal microscopy

HeLa cells were transiently transfected with HA-SHP-1, FLAG-TRAF3, or control vector for 48 hours and fixed with 4% of formaldehyde for 20 minutes at room temperature. Then, cells were permeabilized with PBST (0.3% of Triton X-100 in PBS) for 30 minutes, and nonspecific binding was blocked in blocking buffer (1% of BSA in PBS) for 1 hour at 4°C. After that, cells were incubated with primary antibodies at 4°C overnight and secondary antibodies for 1 hour at room temperature. After staining with 4',6-diamidino-2-phenylindole, images were captured with Leica TCS SP5 confocal laser microscope according to the manufacturer's instructions.

2.11 | RNA interference

RAW264.7 cells were digested with trypsin and counted with cell counter. siRNA targeting SHP-1 and control siRNA were transfected into RAW264.7 cells using the Amaxa program D-032 according to the manufacturer's instructions.

2.12 | Quantitative real-time PCR

Total RNA was extracted with RNAiso Plus (9109; Takara) according to the manufacturer's instructions. One microgram of RNA was reverse transcribed to cDNA using PrimeScript RT reagent kit (RR037; Takara). Quantitative real-time analysis of indicated genes was performed on LightCycler (LC480; Roche) using SYBR RT PCR kit (QPK 212; Toyobo) according to the manufacturer's instructions.

2.13 | Statistical analysis

Statistical analyses included unpaired, two-tailed Student's *t* tests. Data are presented as mean ± SEM from at least three independent experiments. The differences were considered statistically significant at *P* < .05. These statistical analyses were performed using GraphPad Prism 8.

3 | RESULTS

3.1 | Knockout or knockdown of SHP-1 enhances HSV-1- and VSV-induced innate antiviral immune response

Virus infection triggers activation of antiviral signaling pathways and promotes the production of type I IFNs, chemokines, interferon-stimulated genes and proinflammatory cytokines, such as IFN-β, CXCL10, ISG15, and TNF.³¹ To investigate the role of SHP-1 in the innate antiviral immune response, we isolated primary peritoneal macrophages (PMs) from wild-type (WT) and SHP-1 deficient mice (*Ptpn6*^{me-v/me-v}) and infected them with herpes simplex virus 1 (HSV-1) or vesicular stomatitis virus (VSV) for 12 hours. The results indicated that knockout of SHP-1 resulted in elevated levels of transcripts encoding *IFNB*, *CXCL10*, *ISG15*, and *TNF* as revealed by quantitative real-time PCR (qRT-PCR) (Figure 1A,B). Accordingly, the virus titers were significantly decreased in PMs from *Ptpn6*^{me-v/me-v} mice compared with those from WT mice (Figure 1C). To determine the mechanism by which SHP-1 regulates type I IFN production, we examined the phosphorylation of major regulators of antiviral signal transduction at indicated times after HSV-1 infection. Increased phosphorylation of TBK1, IRF3, STAT1, p65, p38, and Erk was observed in *Ptpn6*^{me-v/me-v} PMs compared with those from WT mice (Figure 1D), indicating that SHP-1 inhibits virus-induced signaling in response to infection. We next transfected RAW264.7 with siRNA and found that SHP-1-specific siRNA decreased the expression of SHP-1 (Figure 1E). As expected, knockdown of SHP-1 by siRNA resulted in elevated expression of *IFNB*, *CXCL10*, *ISG15*, and *TNF* (Figure 1F,G) and lower virus

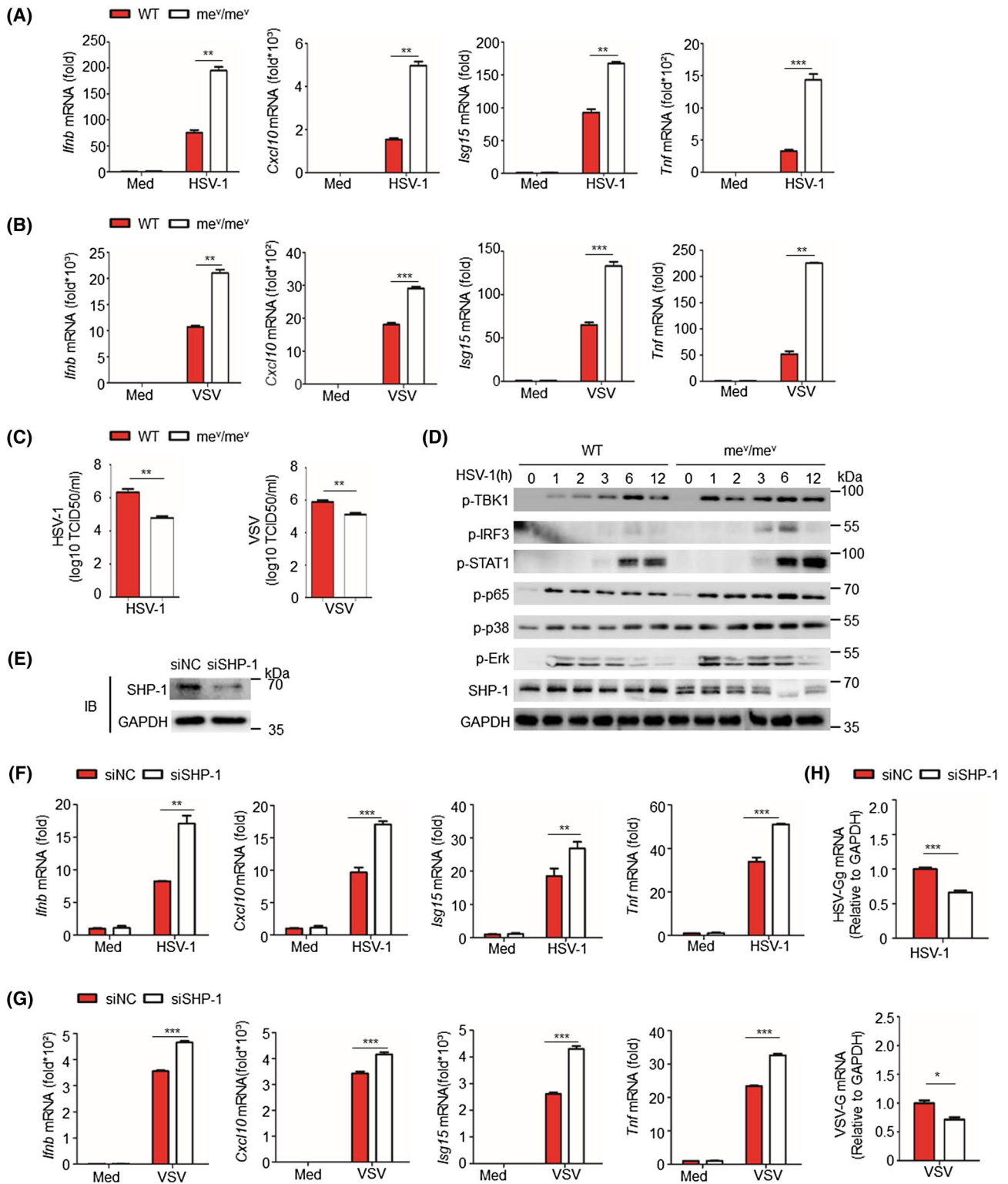


FIGURE 1 Knockout or knockdown of SHP-1 enhances the HSV-1- and VSV-induced innate antiviral immune response. A and B, *IFNB*, *CXCL10*, *ISG15*, and *TNF* mRNA levels (fold-increase relative to uninfected cells treated with medium (Med)) in PMs from WT or *Ptpn6^{me-v/me-v}* mice infected with HSV-1 (A) or VSV (B) for 12 hours. C, virus titers from experiments shown in (A) and (B). D, immunoblot of lysates of PMs from WT or *Ptpn6^{me-v/me-v}* mice infected with HSV-1 at indicated times. E, immunoblot of lysates from RAW264.7 cells transfected with control siRNA or SHP-1-specific siRNA for 24 hours. F and G, *IFNB*, *CXCL10*, *ISG15*, and *TNF* mRNA levels in RAW264.7 cells transfected with control siRNA or SHP-1 siRNA, and then, infected with HSV-1 (F) or VSV (G) for 12 hours. H, virus load from experiments shown in (F) and (G). Data are representative of at least three independent experiments (mean \pm SEM in A-C, F-H). * $P < .05$, ** $P < .01$, and *** $P < .001$, two-tailed unpaired Student's *t* test

load (Figure 1H) in response to HSV-1 or VSV infection. These data suggest that knockout or knockdown SHP-1 enhances host antiviral signaling and type I IFN production in response to infection with DNA or RNA viruses.

3.2 | Overexpression of SHP-1 suppresses HSV-1- and VSV-induced innate antiviral immune response

L929 cells are commonly used in virus-related studies as they produce IFN- β and related proinflammatory cytokines.³² To confirm the impact of SHP-1 on the antiviral immune response, we transfected vector encoding SHP-1

or control vector into L929 cells, and then, infected them with HSV-1 or VSV for 12 hours. We found that overexpression of SHP-1 resulted in a significant decrease in expression of *IFNB*, *CXCL10*, *ISG15*, and *TNF* compared with the control (Figure 2A,B). Moreover, the virus load in L929 cells overexpressing SHP-1 was higher than that in control cells (Figure 2C). These results indicate that SHP-1 suppresses the innate antiviral immune response. To explore the mechanism further, we also examined the phosphorylation of critical signaling regulators at the indicated time points after VSV infection. Consistent with decreased expression of proinflammatory cytokines, overexpression of SHP-1 resulted in markedly reduced phosphorylation of TBK1, IRF3, STAT1, p65, p38, and Erk (Figure 2D). These results suggest

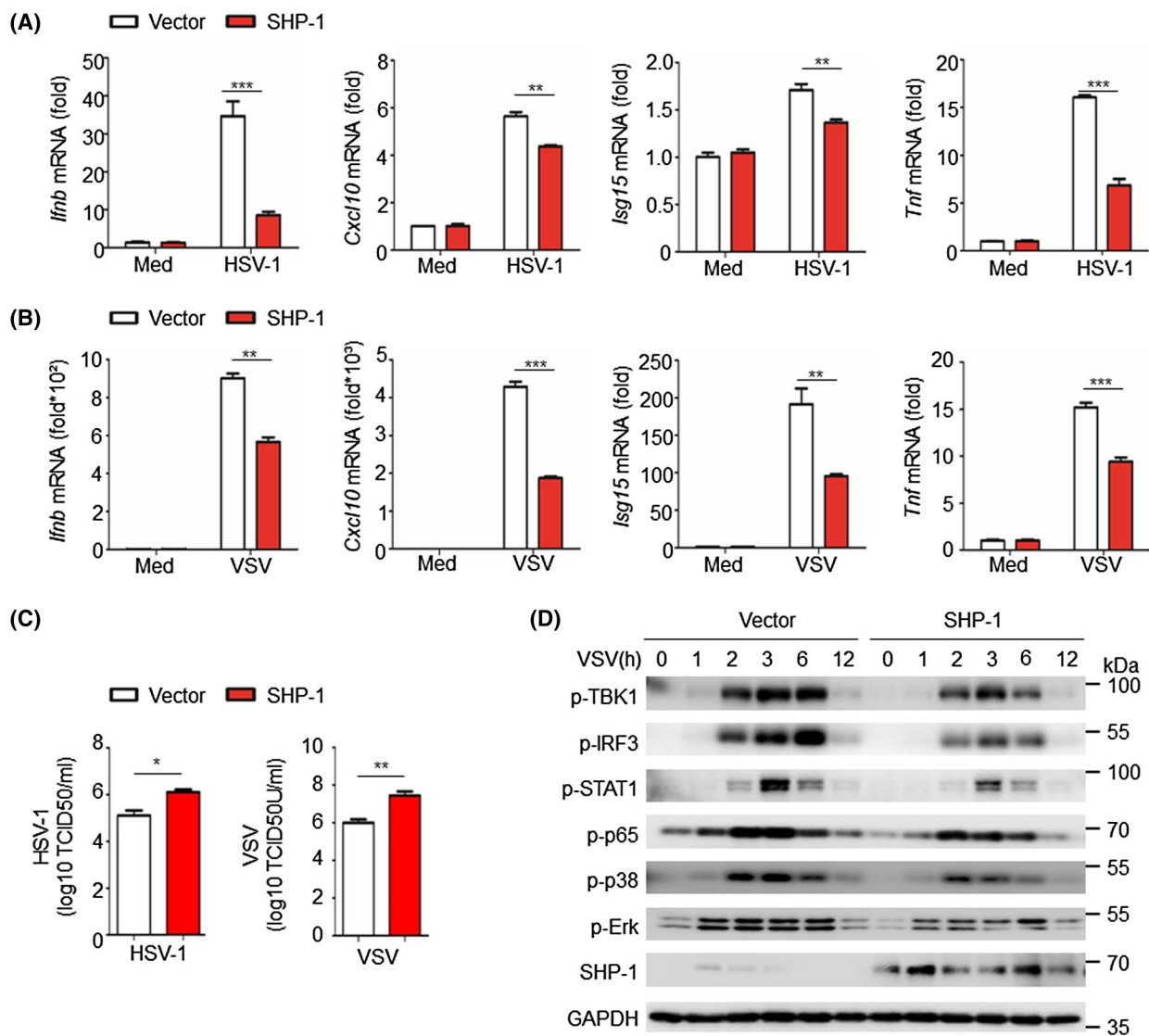


FIGURE 2 Overexpression of SHP-1 suppresses HSV-1- and VSV-induced innate antiviral immune response. A and B, *IFNB*, *CXCL10*, *ISG15*, and *TNF* mRNA levels in L929 cells transfected with control vector or vector encoding SHP-1, and then, infected with HSV-1 (A) or VSV (B) for 12 hours. C, the virus titers from experiments as in (A) and (B). D, immunoblot of lysates of L929 transfected with control vector or SHP-1 and infected with VSV at indicated times. Data are representative of at least three independent experiments (mean \pm SEM in A-C). * $P < .05$, ** $P < .01$, and *** $P < .001$, two-tailed unpaired Student's t test

that overexpression of SHP-1 inhibits host antiviral signaling transduction and type I IFN production in response to DNA or RNA virus infection.

3.3 | SHP-1-mediated immune inhibition requires phosphatase activity

SHP-1 is a PTP with two SH2 domains and phosphatase activity that is dependent on the amino acid Cys⁴⁵³. To determine whether SHP-1-mediated immune inhibition is dependent on its phosphatase activity, we generated the SHP-1 mutant (SHP-1^{C453S}), in which the cysteine at position 453 was replaced with serine. The WT SHP-1 and SHP-1^{C453S} were detected at comparable levels when expressed in L929 cell transfectants (Figure 3A). L929 cells were transfected with control vector, SHP-1, or SHP-1^{C453S} and infected with HSV-1 or VSV for 12 hours. Interestingly, cells transfected with SHP-1^{C453S} were unable to inhibit expression of

IFNB, *CXCL10*, *ISG15*, and *TNF* (Figure 3B,C). Moreover, the virus titer from SHP-1^{C453S}-transfected cells was lower than that from the SHP-1-transfected cells and comparable with titers from control cells (Figure 3D). These data suggest that SHP-1 may suppress type I IFN production through its phosphatase activity and indicate that SHP-1 might serve as a negative regulator of the host antiviral immune response by dephosphorylating critical tyrosine residues in intracellular signaling molecules.

3.4 | SHP-1 interacts with TRAF3

To explore further the molecular mechanism by which SHP-1 suppresses the antiviral immune response, we performed luciferase assays in HEK293T cells.^{33,34} Among the results, we showed that SHP-1 suppressed N-RIG-I-, MAVS-, and TRAF3/TBK1-mediated induction of the antiviral immune response but had no impact on TBK1- and

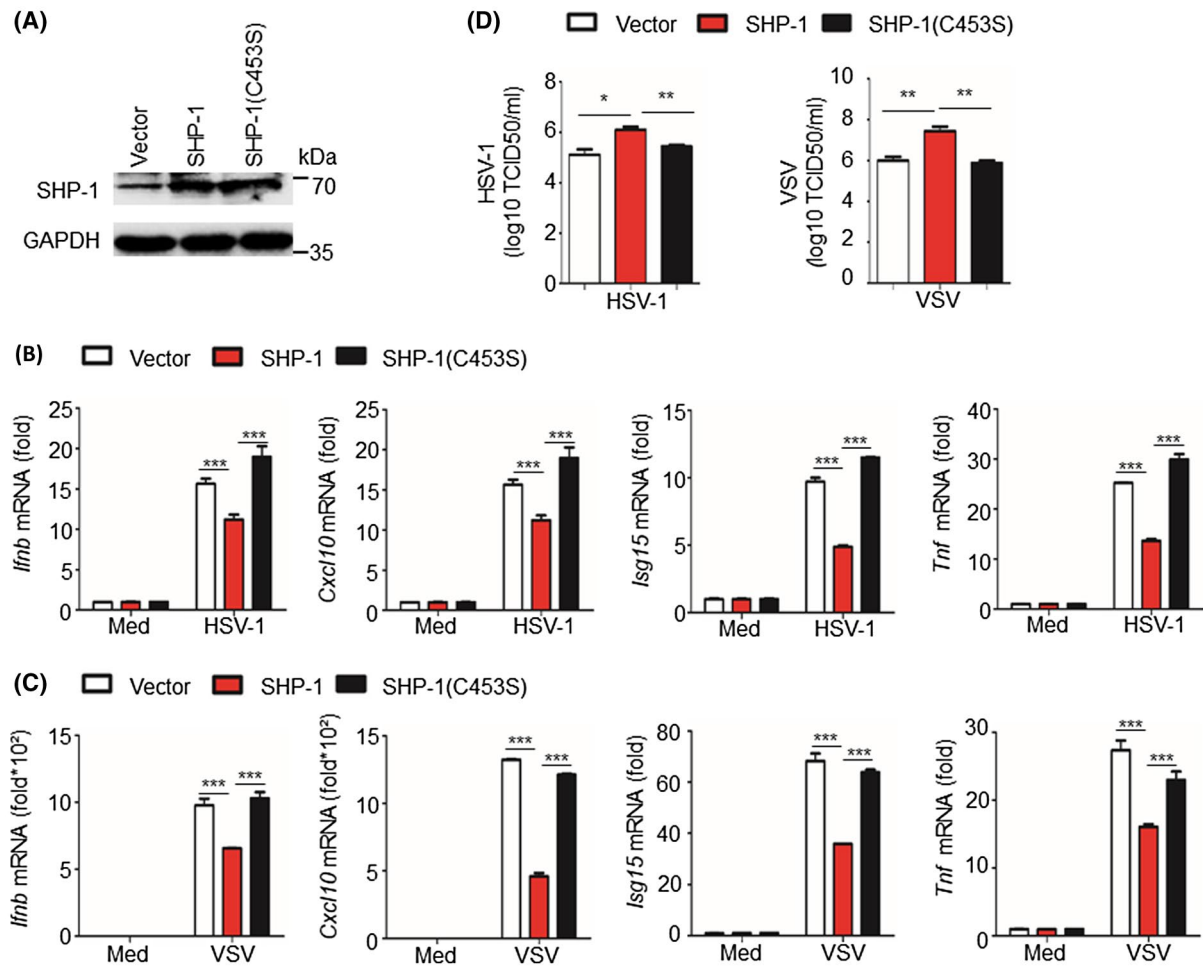


FIGURE 3 SHP-1-mediated immune inhibition requires phosphatase activity. A, immunoblot of lysates of L929 cells transfected with control vector or vectors encoding SHP-1 or SHP-1^{C453S}. B and C, *IFNB*, *CXCL10*, *ISG15*, and *TNF* mRNA levels in L929 cells transfected with control vector or vectors encoding SHP-1 or SHP-1^{C453S} and infected with HSV-1 (B) or VSV (C) for 12 hours. D, virus titers from experiments in (B) and (C). Data are representative of at least three independent experiments (mean ± SEM in B-D). **P* < .05, ***P* < .01, and ****P* < .001, two-tailed unpaired Student's *t* test

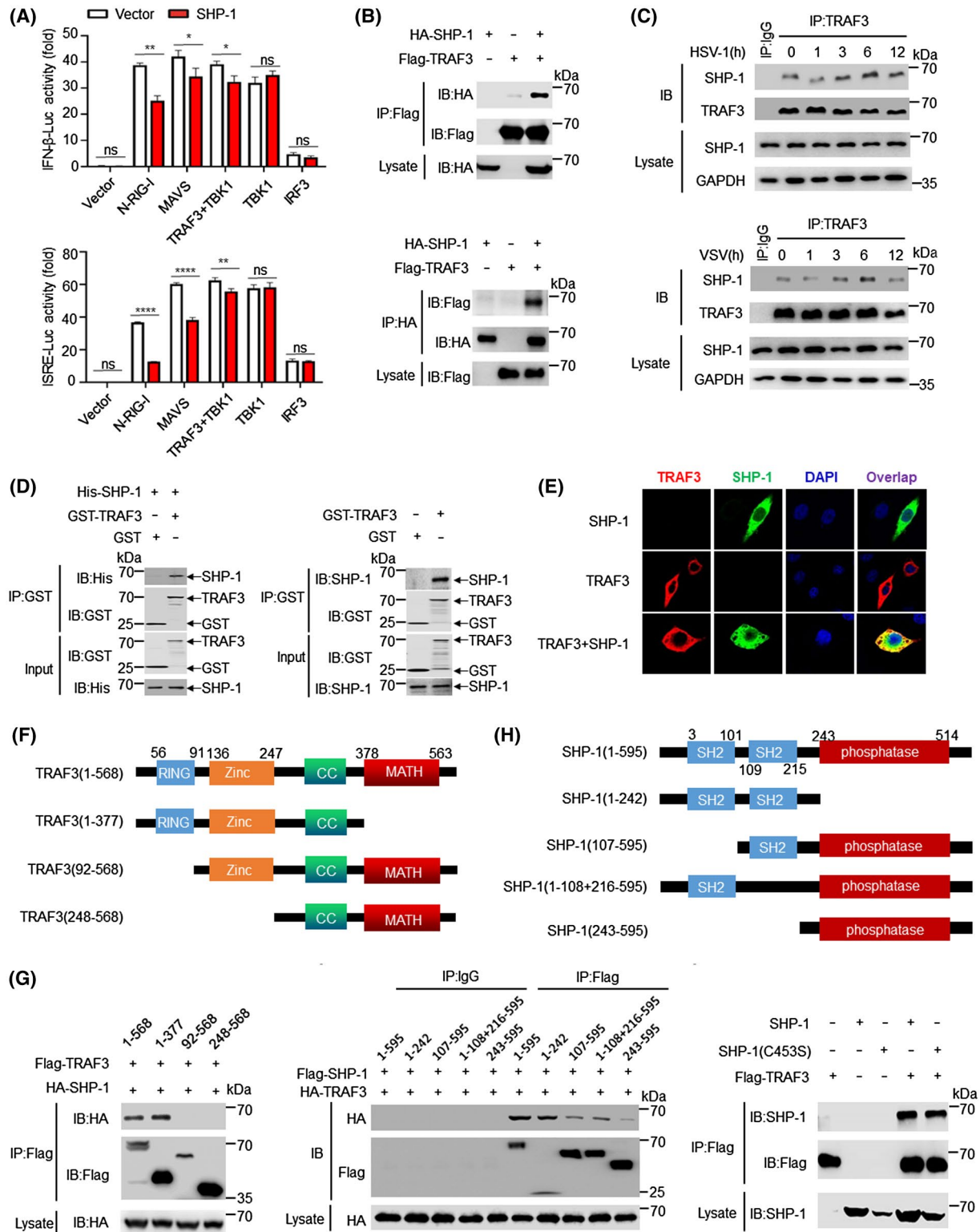


FIGURE 4 SHP-1 interacts with TRAF3. A, luciferase assay of IFN- β and ISRE activation in HEK293T cells expressing N-RIG-I, MAVS, TBK1, TRAF3, IRF3, and SHP-1 or transfected with control vector. B, immunoprecipitation and immunoblot analysis of lysates of HEK293T cells transfected with vectors as indicated. C, immunoprecipitation and immunoblot analysis of lysates of PMs from WT mice infected with HSV-1 or VSV at indicated times. D, direct binding of GST-TRAF3 with His-SHP-1 (left) or endogenous SHP-1 from PMs (right). E, confocal image of HeLa cells transfected with vectors encoding SHP-1 and TRAF3. F, deletion mutants of TRAF3. G, immunoprecipitation and immunoblot analysis of lysates of HEK293T cells transfected with vectors as indicated. H, deletion mutants of SHP-1. I, immunoprecipitation and immunoblot analysis of lysates of HEK293T cells expressing various vectors (above lanes). Data are representative of at least three independent experiments (mean \pm SEM in A). * P < .05, ** P < .01, and **** P < .0001, two-tailed unpaired Student's t test

IRF3-induced activation of IFN- β and interferon-stimulated response elements (ISREs) (Figure 4A). These results indicated that SHP-1 might participate in an inhibitory role at a point upstream of TBK1-IRF3. Furthermore, we found that SHP-1 interacted with TRAF3 by forward and reverse co-immunoprecipitation (Co-IP) assays (Figure 4B). Meanwhile, we examined the interaction of endogenous SHP-1 and TRAF3 in PMs and the results showed that these two proteins interact with each other in PMs, while HSV-1 and VSV infection facilitated their interaction (Figure 4C). To determine whether SHP-1 binds to TRAF3 directly, we purified glutathione-S-transferase (GST)-TRAF3 and His-SHP-1 with GST-beads and Ni-column, respectively, from BL-21 bacteria and then, incubated them together, or incubated GST-TRAF3 with lysates from primary PMs. The GST pull-down assay revealed that both purified and endogenous SHP-1 could bind directly to TRAF3 (Figure 4D). Furthermore, immunofluorescence confocal microscopy analysis showed that SHP-1 co-localized with TRAF3 in transfected HeLa cells (Figure 4E).

To determine the nature of the interaction between SHP-1 and TRAF3, we analyzed the interaction of SHP-1 with various deletion mutants of TRAF3 (Figure 4F), including those targeting the N-terminal RING finger, the zinc finger, and the C-terminal MATH domains. By Co-IP experiments, we determined that the interactions of TRAF3(92-568) and TRAF3(248-568) with SHP-1 were almost totally blocked compared with full-length TRAF3 and TRAF3 (1-377). These results indicate that the region containing RING finger (containing amino acids 56-91) is essential for interactions between TRAF3 and SHP-1 (Figure 4G). Similarly, we analyzed the domains of SHP-1, which included two SH2 domains and one phosphatase activity domain (Figure 4H). We found that deletion of either N-terminal SH2 domain or C-terminal SH2 domain resulted in less coimmunoprecipitation of TRAF3 with SHP-1, whereas deletion of both SH2 domains resulted much less interaction still (Figure 4I), suggesting that the interaction between TRAF3 and SHP-1 was to large extent dependent on the SH2 domains of SHP-1. To test whether the interaction between SHP-1 and TRAF3 was dependent on its phosphatase activity, we transfected HEK293T cells with plasmids encoding TRAF3 and SHP-1 or SHP-1^{C453S} and found that the phosphatase activity of SHP-1 was not necessary to promote or maintain the interaction between these two proteins (Figure 4J).

3.5 | SHP-1 inhibits K63-linked ubiquitination of TRAF3

Ubiquitylation is a posttranslational modification that plays an important role in regulating innate immune response.^{4,35}

Earlier publications reported that K63-linked ubiquitination of TRAF3 promotes the recruitment of TBK1 to MAVS, which is crucial for production of type I IFNs.³⁶ Moreover, the interactions between CK1 ϵ and TRAF3 have been shown to promote K63-linked ubiquitination of TRAF3 by phosphorylating TRAF3 at Ser^{349,37}. To explore the role of SHP-1 and its direct impact on TRAF3 ubiquitination, we first examined the effect of SHP-1 on the interactions between TRAF3 and CK1 ϵ in HEK293T. The results of our Co-IP assay indicated that SHP-1 was able to disrupt the interaction between CK1 ϵ and TRAF3 in a dose-dependent manner and this was accompanied by an apparent decreased phosphorylation of TRAF3. Interestingly, loss of enzymatic activity of SHP-1^{C453S} could not inhibit the interaction of CK1 ϵ and TRAF3 and the phosphorylation of TRAF3, suggesting that SHP-1-induced inhibition of the interaction is dependent on its phosphatase activity (Figure 5A). Simultaneously, we examined the interaction of endogenous CK1 ϵ and TRAF3 in WT and *Ptpn6*^{me-v/me-v} mice upon VSV infection, and the results showed stronger binding of CK1 ϵ and TRAF3 in *Ptpn6*^{me-v/me-v} PMs compared to WT PMs (Figure 5B). Together, we confirmed that SHP-1 could significantly inhibit the interaction of CK1 ϵ with TRAF3.

We next explored whether SHP-1 inhibits ubiquitination of TRAF3 by transfecting HEK293T cells with vectors expressing TRAF3, CK1 ϵ , and HA-Ub with SHP-1 or control vector. We observed that SHP-1 markedly reduced CK1 ϵ -induced ubiquitination of TRAF3 in a dose-dependent manner (Figure 5C). Similarly, we used vectors of HA-K63-Ub and HA-K48-Ub, in which all lysines were mutated to arginine except for Arg63 or Arg48 and found that overexpression of SHP-1 also resulted in diminished K63-linked ubiquitination of TRAF3 (Figure 5D) but had no impact on K48-linked ubiquitination (Figure 5E). We next examined the ubiquitination of endogenous TRAF3 in PMs from WT and *Ptpn6*^{me-v/me-v} mice upon VSV infection and found that knockout of SHP-1 promoted the total and K63-linked ubiquitination of TRAF3 but had no significant effect on K48-linked ubiquitination (Figure 5F).

Subsequently, we confirmed whether the inhibition of K63 ubiquitination of TRAF3 by SHP-1 was dependent on its phosphatase activity. The Co-IP assays indicated that SHP-1^{C453S} abrogated inhibition of K63-linked ubiquitination of TRAF3 (Figure 5G). These results indicated that the phosphatase activity of SHP-1 is a critical for the inhibition of K63-linked ubiquitination of TRAF3. K63-linked ubiquitination of TRAF3 is essential for its binding to TBK1.^{22,38} As anticipated, overexpression of SHP-1 resulted in a dramatic, dose-dependent inhibition of the interaction between TRAF3 and TBK1, while SHP-1^{C453S} lost the ability to inhibit the binding of TRAF3 to TBK1 (Figure 5H). Furthermore, we found that SHP-1 promoted a decrease in

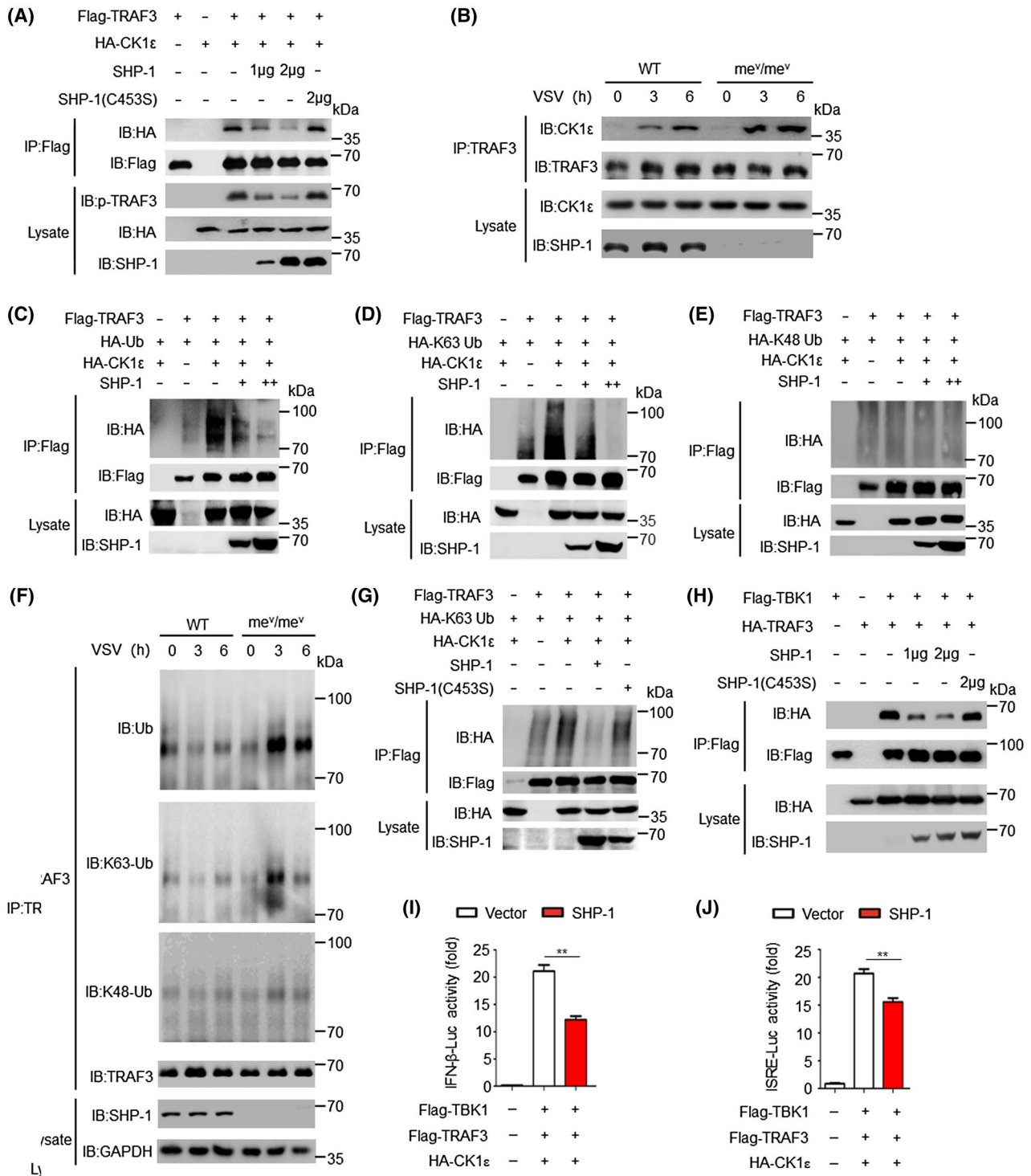


FIGURE 5 SHP-1 inhibits K63-linked ubiquitination of TRAF3. A, immunoprecipitation and immunoblot analysis of lysates of HEK293T cells transfected with vectors as indicated. B, immunoprecipitation and immunoblot analysis of lysates of PMs from WT and *Ptpn6*^{me-v/me-v} mice infected with VSV at indicated times. C-E, immunoprecipitation and immunoblot analysis of lysates of HEK293T cells transfected with vectors as indicated. F, immunoprecipitation and immunoblot analysis of lysates of PMs from WT and *Ptpn6*^{me-v/me-v} mice infected with VSV at indicated times. G and H, immunoprecipitation and immunoblot analysis of lysates of HEK293T cells transfected with vectors as indicated. I and J, luciferase assay of IFN-β (I) and ISRE (J) activation in HEK293T cells transfected with vectors as indicated. Data are representative of at least three independent experiments (mean ± SEM in I and J). ***P* < .01, two-tailed unpaired Student's *t* test

TBK1-TRAF3-CK1ε-induced IFN-β and ISRE activation by luciferase assay (Figure 5I,J). These data suggest that SHP-1 inhibits K63-linked ubiquitination of TRAF3, and thereby

disrupts the binding of TBK1 and TRAF3; this results in impaired downstream signaling and a reduction in the synthesis of type I IFNs.

3.6 | SHP-1 targets TRAF3 at Tyr116 and Tyr446 to inhibit its K63-linked ubiquitination

We have confirmed that the inhibitory role of SHP-1 on K63-linked ubiquitination of TRAF3 is dependent on its phosphatase activity. Here, we raised the hypothesis that, as a PTP, SHP-1 might dephosphorylate TRAF3 at a tyrosine residue and thereby, negatively regulate its K63-linked ubiquitination. To validate this hypothesis, we first detected

the effect of virus infection on TRAF3 tyrosine phosphorylation in PMs and found that HSV-1 and VSV infection significantly promoted tyrosine phosphorylation of TRAF3 (Figure 6A). Since the SRC-family tyrosine kinase can specifically catalyze tyrosine phosphorylation, we constructed six eukaryotic expression vectors of SRC-family (BLK, FRK, FYN, LCK, LYN, and SRC) and further identified tyrosine kinases involved in TRAF3 tyrosine phosphorylation. The Co-IP assays displayed that only BLK could specifically

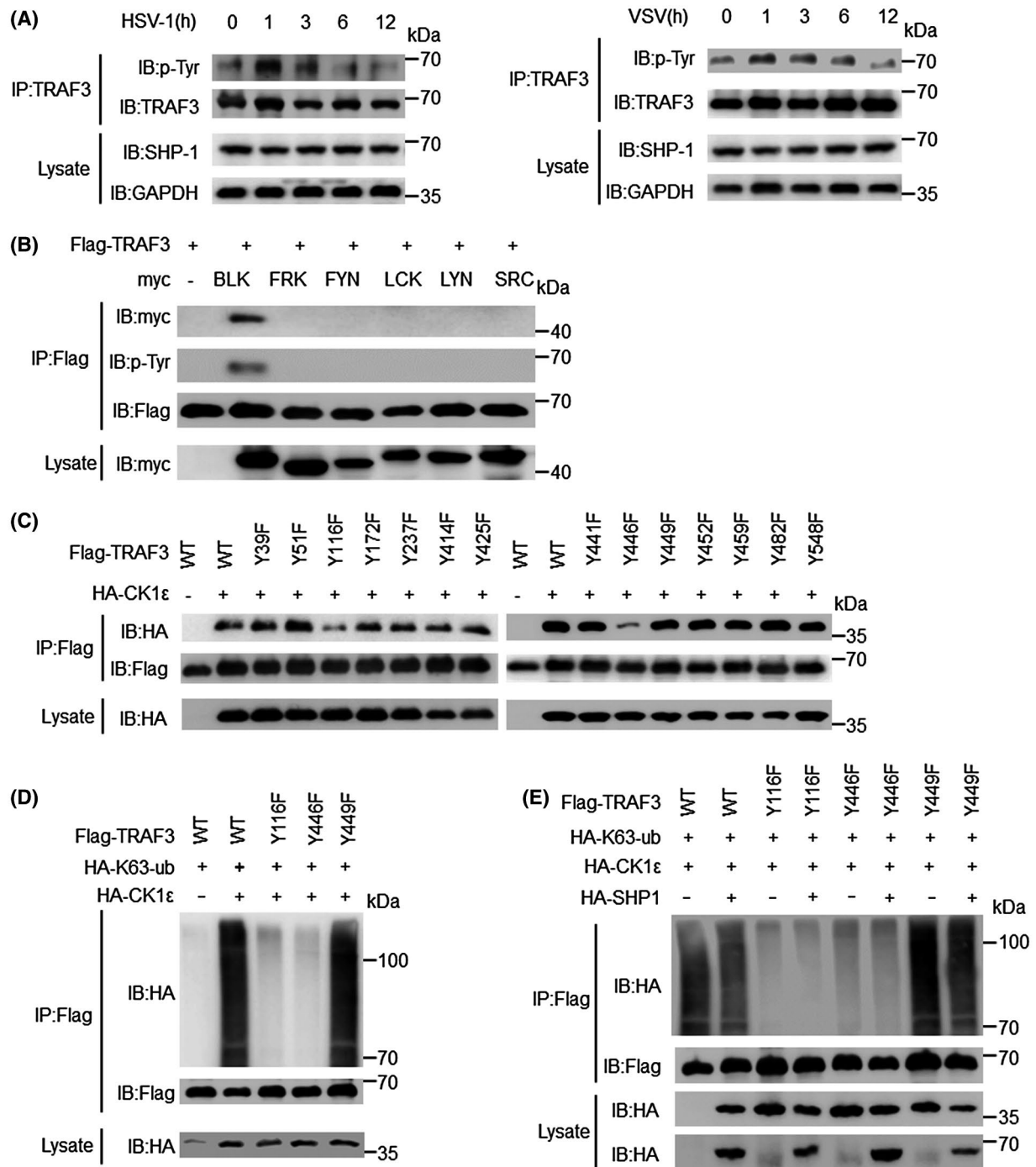


FIGURE 6 SHP-1 targets TRAF3 at Tyr116 and Tyr446 to inhibit its K63-linked ubiquitination. A-E, immunoprecipitation and immunoblot analysis of lysates of HEK293T cells transfected with vectors as indicated. Data are representative of at least three independent experiments

targeted to TRAF3 and promoted its tyrosine phosphorylation (Figure 6B).

To further investigate the mechanism by which TRAF3 tyrosine regulates its ubiquitination, we generated mutations (to phenylalanine) at the 14 tyrosine residues in TRAF3. Interestingly, we found that the interaction of CK1 ϵ with TRAF3^{Y116F}, TRAF3^{Y446F} were markedly decreased compared with interactions with WT TRAF3 by Co-IP (Figure 6C); as expected, TRAF3^{Y116F} and TRAF3^{Y446F} mutants exhibited reduced K63-linked ubiquitination (Figure 6D). These data suggest that the phosphorylation of TRAF3 at Tyr 116 and Tyr 446 regulate CK1 ϵ -induced K63-linked ubiquitination. To confirm whether SHP-1 inhibited K63-linked ubiquitination of TRAF3 by targeting tyrosine, we overexpressed SHP-1 together with HA-K63 Ub, HA-CK1 ϵ , and Flag-TRAF3 and related mutant proteins in HEK293T cells. We found that SHP-1 did not promote additional decrease in K63-linked ubiquitination of TRAF3^{Y116F} and TRAF3^{Y446F} but did decrease K63-linked ubiquitination of WT TRAF3 and the TRAF3^{Y449F} mutant (Figure 6E). These results indicate that SHP-1 inhibit K63-linked ubiquitination of TRAF3 by dephosphorylating it at Tyr116 and Tyr446. Collectively, these results suggest that SHP-1 suppress K63-linked ubiquitination of TRAF3 by dephosphorylating it at Tyr116 and Tyr446.

4 | DISCUSSION

SHP-1 is a critical negative regulator in a variety of signaling pathways and plays important roles in human diseases as well as various disorders modeled in mice.³⁹⁻⁴¹ The basic function of SHP-1 is to dephosphorylate kinases and suppress signal activation in a variety of intracellular pathways.^{42,43} SHP-1 also promotes negative regulation of signal transduction and immune responses to bacterial infection.^{29,44,45} However, there is relatively little evidence that suggests a role for SHP-1 in response to virus infection. The results from our study identified SHP-1 as an inhibitory regulator that suppressed antiviral signal transduction and type I IFN production in L929 cells, primary macrophages, and RAW264.7 cells in response to infection with HSV-1 or VSV; this activity was directly dependent on its endogenous phosphatase activity. Furthermore, we demonstrated that SHP-1 directly interacted with TRAF3 and resulted in diminished K63-linked ubiquitination by catalyzing its dephosphorylation at Tyr116 and Tyr446. This serves to obstruct TRAF3-TBK1 complex formation, thereby impairing downstream signal activation and type I IFN production.

As we know, ubiquitin mainly binds to lysine residues in specific substrates and thereby has an impact on their stability and/or activity. K48-linked ubiquitination typically mediates protein degradation, and K63-linked ubiquitination mediates protein activation.^{33,34,46} In our study, we demonstrated that

SHP-1 obstructs antiviral signal transduction by disrupting K63-linked ubiquitination of TRAF3; we identified two key tyrosine residues at Tyr116 and Tyr446 that might be targets of SHP-1. However, we are still not certain of the mechanistic endpoint of TRAF3 ubiquitination in this pathway. It will be necessary to elucidate the specific lysine in TRAF3 that was targeted by SHP-1 and to explore whether Tyr116 and/or Tyr446 are/is involved in the regulation of K63-linked ubiquitination. In the meantime, it is interesting to further clarify the roles of specific lysine residues with respect to signal transduction and type I IFN production in response to HSV-1 or VSV infection. K63-linked ubiquitination of TRAF3 is positively regulated by the conserved serine-threonine kinase CK1 ϵ .³⁷ Moreover, cellular inhibitor of apoptosis protein (cIAP)1 and cIAP2, two E3 ubiquitin ligases, interact with TRAF3 upon virus infection and promote K63-linked ubiquitination of TRAF3 to stimulate IRF3 activation and IFN- β production.⁴⁷ In our study, we found SHP-1 directly bound to TRAF3 and inhibited the interaction of CK1 ϵ and TRAF3, which subsequently suppressed CK1 ϵ -induced K63-linked ubiquitination of this target. At this time, we cannot exclude the possibility that SHP-1 might suppress an interaction between TRAF3 with cIAP1 or cIAP2, which may then form a complex with CK1 ϵ during virus infection. We will need to determine whether SHP-1 is capable of disrupting interactions between TRAF3 and the E3 ubiquitin ligases, as these findings will further illuminate the suppressive molecular mechanism of SHP-1 and its complex roles in modulating the innate antiviral immune response.

Previous publications have reported that SHP-1 promoted macrophage recruitment, notably in response to infection with Theiler's encephalomyelitis virus;⁴⁸ however, no evidence was provided suggesting that SHP-1 participated in macrophage activation in response to virus infection. Our study clearly demonstrated that SHP-1 inhibited the cytokine production including type I IFNs in macrophages by targeting TRAF3. We suspect that SHP-1 may also have a significant impact on the expression of chemokines and/or chemokine receptors that may ultimately obstruct the recruitment of macrophages. Moreover, SHP-1 is broadly expressed in numerous immune cells including neutrophils, DCs, monocytes, and macrophages; all of these cells have pivotal roles in promoting antiviral immune responses. Further exploration of the interactions between SHP-1 and TRAF3 in other immune cells will be a critical next step. Taken together, our results demonstrated that SHP-1 serves as a negative regulator of the antiviral immune response by suppressing K63-linked ubiquitination of TRAF3, an action that may be mediated by dephosphorylation of TRAF3 at Tyr116 and Tyr446. These findings provide a mechanistic explanation for immune evasion and highlight potential therapeutic targets for the treatment of virus infection.

ACKNOWLEDGMENTS

This work was supported by grants from the National Natural Science Foundation of China (project 31972900 and 31670901), Innovative Research Team of High-level Local Universities in Shanghai, the Program for Professor of Special Appointment (Eastern Scholar) at Shanghai Institutions of Higher Learning (program TP2016007), the Outstanding Youth Training Program of Shanghai Municipal Commission of Health and Family Planning (program 2017YQ012), the National Key Research and Development Program of China (program 2016YFC1305103 and 2018YFC1705505) and the National megaproject on key infectious diseases (program 2017ZX10202102). We thank Dr X. Cao (Chinese Academy of Medical Sciences) for generously providing Ptpn6^{me-v}/me-v mice, Dr J. Xu (Shanghai Public Health Clinical Center) for providing the Vero cell line; and all members of Yan lab for helpful discussions and suggestions.

CONFLICT OF INTEREST

The authors declare no conflicts of interest.

AUTHOR CONTRIBUTIONS

D. Hao, Y. Wang, and D. Yan designed and conducted the experiments; D. Hao, Y. Wang, L. Li, G. Qian, J. Liu, M. Li, Y. Zhang, and R. Zhou provided reagents and methods; D. Hao and Y. Wang analyzed the data and wrote the manuscript; D. Yan supervised the study and edited the manuscript; D. Yan provided financial support; and all authors read and approved the manuscript.

REFERENCES

1. Towers GJ, Noursadeghi M. Interactions between HIV-1 and the cell-autonomous innate immune system. *Cell Host Microbe*. 2014;16:10-18.
2. Liu ZY, Shi WF, Qin CF. The evolution of Zika virus from Asia to the Americas. *Nat Rev Microbiol*. 2019;17:131-139.
3. Li H, Ying T, Yu F, Lu L, Jiang S. Development of therapeutics for treatment of Ebola virus infection. *Microbes Infect*. 2015;17:109-117.
4. Hutchinson EC. Influenza virus. *Trends Microbiol*. 2018;26:809-810.
5. The L. Emerging understandings of 2019-nCoV. *Lancet*. 2020;395:311.
6. Holshue ML, DeBolt C, Lindquist S, et al. First case of 2019 novel coronavirus in the United States. *N Engl J Med*. 2020;382:929-936.
7. Rothe C, Schunk M, Sothmann P, et al. Transmission of 2019-nCoV infection from an asymptomatic contact in Germany. *N Engl J Med*. 2020;382:970-971.
8. Wang M, Cao R, Zhang L, et al. Remdesivir and chloroquine effectively inhibit the recently emerged novel coronavirus (2019-nCoV) in vitro. *Cell Res*. 2020;30:269-271.
9. Zhao W. Negative regulation of TBK1-mediated antiviral immunity. *FEBS Lett*. 2013;587:542-548.
10. O'Neill LA. When signaling pathways collide: positive and negative regulation of toll-like receptor signal transduction. *Immunity*. 2008;29:12-20.
11. Medzhitov R, Janeway CA, Jr. Decoding the patterns of self and nonself by the innate immune system. *Science*. 2002;296:298-300.
12. Akira S, Takeda K. Toll-like receptor signalling. *Nat Rev Immunol*. 2004;4:499-511.
13. Zhao B, Shu C, Gao X, et al. Structural basis for concerted recruitment and activation of IRF-3 by innate immune adaptor proteins. *Proc Natl Acad Sci U S A*. 2016;113:E3403-E3412.
14. Seth RB, Sun L, Chen ZJ. Antiviral innate immunity pathways. *Cell Res*. 2006;16:141-147.
15. Yoneyama M, Kikuchi M, Natsukawa T, et al. The RNA helicase RIG-I has an essential function in double-stranded RNA-induced innate antiviral responses. *Nat Immunol*. 2004;5:730-737.
16. Radoshevich L, Dussurget O. Cytosolic innate immune sensing and signaling upon infection. *Front Microbiol*. 2016;7:313.
17. Liu S, Cai X, Wu J, et al. Phosphorylation of innate immune adaptor proteins MAVS, STING, and TRIF induces IRF3 activation. *Science*. 2015;347:aaa2630.
18. Wu J, Sun L, Chen X, et al. Cyclic GMP-AMP is an endogenous second messenger in innate immune signaling by cytosolic DNA. *Science*. 2013;339:826-830.
19. Sun L, Wu J, Du F, Chen X, Chen ZJ. Cyclic GMP-AMP synthase is a cytosolic DNA sensor that activates the type I interferon pathway. *Science*. 2013;339:786-791.
20. Zhang C, Shang G, Gui X, Zhang X, Bai XC, Chen ZJ. Structural basis of STING binding with and phosphorylation by TBK1. *Nature*. 2019;567:394-398.
21. Hacker H, Tseng PH, Karin M. Expanding TRAF function: TRAF3 as a tri-faced immune regulator. *Nat Rev Immunol*. 2011;11:457-468.
22. Oganessian G, Saha SK, Guo B, et al. Critical role of TRAF3 in the Toll-like receptor-dependent and -independent antiviral response. *Nature*. 2006;439:208-211.
23. Kim SS, Lee KG, Chin CS, et al. DOK3 is required for IFN-beta production by enabling TRAF3/TBK1 complex formation and IRF3 activation. *J Immunol*. 2014;193:840-848.
24. Mao HT, Wang Y, Cai J, et al. HACE1 negatively regulates virus-triggered type I IFN signaling by impeding the formation of the MAVS-TRAF3 complex. *Viruses*. 2016;8:146.
25. Matthyys VS, Cimica V, Dalrymple NA, Glennon NB, Bianco C, Mackow ER. Hantavirus GnT elements mediate TRAF3 binding and inhibit RIG-I/TBK1-directed beta interferon transcription by blocking IRF3 phosphorylation. *J Virol*. 2014;88:2246-2259.
26. Chen X, Yang X, Zheng Y, Yang Y, Xing Y, Chen Z. SARS coronavirus papain-like protease inhibits the type I interferon signaling pathway through interaction with the STING-TRAF3-TBK1 complex. *Protein Cell*. 2014;5:369-381.
27. Garg M, Wahid M, Khan FD. Regulation of peripheral and central immunity: understanding the role of Src homology 2 domain-containing tyrosine phosphatases, SHP-1 & SHP-2. *Immunobiology*. 2019;225:151847.
28. Abram CL, Lowell CA. Shp1 function in myeloid cells. *J Leukoc Biol*. 2017;102:657-675.
29. Zhou R, Chen Z, Hao D, et al. Enterohemorrhagic *Escherichia coli* Tir inhibits TAK1 activation and mediates immune evasion. *Emerg Microbes Infect*. 2019;8:734-748.
30. Yan D, Wang X, Luo L, Cao X, Ge B. Inhibition of TLR signaling by a bacterial protein containing immunoreceptor tyrosine-based inhibitory motifs. *Nat Immunol*. 2012;13:1063-1071.
31. Doyle T, Goujon C, Malim MH. HIV-1 and interferons: who's interfering with whom? *Nat Rev Microbiol*. 2015;13:403-413.

32. Varble AJ, Ried CD, Hammond WJ, Marquis KA, Woodruff MC, Ferran MC. The vesicular stomatitis virus matrix protein inhibits NF-kappaB activation in mouse L929 cells. *Virology*. 2016;499:99-104.
33. Tsuchida T, Zou J, Saitoh T, et al. The ubiquitin ligase TRIM56 regulates innate immune responses to intracellular double-stranded DNA. *Immunity*. 2010;33:765-776.
34. Zhang J, Hu MM, Wang YY, Shu HB. TRIM32 protein modulates type I interferon induction and cellular antiviral response by targeting MITA/STING protein for K63-linked ubiquitination. *J Biol Chem*. 2012;287:28646-28655.
35. Davis ME, Gack MU. Ubiquitination in the antiviral immune response. *Virology*. 2015;479-480:52-65.
36. Zhang L, Liu J, Qian L, et al. Induction of OTUD1 by RNA viruses potently inhibits innate immune responses by promoting degradation of the MAVS/TRAF3/TRAF6 signalosome. *PLoS Pathog*. 2018;14:e1007067.
37. Zhou Y, He C, Yan D, et al. The kinase CK1 varepsilon controls the antiviral immune response by phosphorylating the signaling adaptor TRAF3. *Nat Immunol*. 2016;17:397-405.
38. Wang S, Wang K, Li J, Zheng C. Herpes simplex virus 1 ubiquitin-specific protease UL36 inhibits beta interferon production by deubiquitinating TRAF3. *J Virol*. 2013;87:11851-11860.
39. Zhu Z, Oh SY, Cho YS, Zhang L, Kim YK, Zheng T. Tyrosine phosphatase SHP-1 in allergic and anaphylactic inflammation. *Immunol Res*. 2010;47:3-13.
40. Zhang Q, Wang HY, Marzec M, Raghunath PN, Nagasawa T, Wasik MA. STAT3- and DNA methyltransferase 1-mediated epigenetic silencing of SHP-1 tyrosine phosphatase tumor suppressor gene in malignant T lymphocytes. *Proc Natl Acad Sci U S A*. 2005;102:6948-6953.
41. Khoury JD, Rassidakis GZ, Medeiros LJ, Amin HM, Lai R. Methylation of SHP1 gene and loss of SHP1 protein expression are frequent in systemic anaplastic large cell lymphoma. *Blood*. 2004;104:1580-1581.
42. Christophi GP, Panos M, Hudson CA, et al. Macrophages of multiple sclerosis patients display deficient SHP-1 expression and enhanced inflammatory phenotype. *Lab Invest*. 2009;89:742-759.
43. Lorenz U. SHP-1 and SHP-2 in T cells: two phosphatases functioning at many levels. *Immunol Rev*. 2009;228:342-359.
44. Nandan D, Knutson KL, Lo R, Reiner NE. Exploitation of host cell signaling machinery: activation of macrophage phosphotyrosine phosphatases as a novel mechanism of molecular microbial pathogenesis. *J Leukoc Biol*. 2000;67:464-470.
45. Rikihisa Y, Lin M. Anaplasma phagocytophilum and Ehrlichia chaffeensis type IV secretion and Ank proteins. *Curr Opin Microbiol*. 2010;13:59-66.
46. Oshiumi H, Matsumoto M, Seya T. Ubiquitin-mediated modulation of the cytoplasmic viral RNA sensor RIG-I. *J Biochem*. 2012;151:5-11.
47. Mao AP, Li S, Zhong B, et al. Virus-triggered ubiquitination of TRAF3/6 by cIAP1/2 is essential for induction of interferon-beta (IFN-beta) and cellular antiviral response. *J Biol Chem*. 2010;285:9470-9476.
48. Watson NB, Schneider KM, Massa PT. SHP-1-dependent macrophage differentiation exacerbates virus-induced myositis. *J Immunol*. 2015;194:2796-2809.

How to cite this article: Hao D, Wang Y, Li L, et al. SHP-1 suppresses the antiviral innate immune response by targeting TRAF3. *The FASEB Journal*. 2020;34:12392–12405. <https://doi.org/10.1096/fj.202000600RR>